# Searching for Asteroids using 8$\mu$m Spitzer Space Telescope Data

Ben Mohlie

## 1. Abstract

Previous studies have estimated the number of asteroids with diameters greater than 1km, but this number varies greatly in different papers and few predictions have been made about the number of asteroids with diameters smaller than 1km. This paper uses data from the Spitzer Space Telescope to look for asteroids in 8$\mu$m images. Two asteroids are found in the Spitzer dark spots. The number of asteroids per deg$^2$ found in this paper agrees with the number of asteroids per deg$^2$ with diameters larger than 1 km predicted by data from the SDSS Moving Object Catalog.

## 2. Introduction

There have been multiple papers discussing the number of asteroids with diameters greater than 1 km, but few attempts have been made to extend estimates to asteroids smaller than 1 km. There is disagreement about the population of asteroids with diameters greater than 1 km. In fact these population estimates can vary by a factor of ten. Three such population estimates are $3 \times 10^5$ (Evans R. et al. 1998), $7 \times 10^5$ (Ivezic et al. 2002), and $1.9 \times 10^6$ (Tedesco et al. 2005). One of the goals of this research is to compare the population estimates of asteroids with a diameter greater than 1 km with the asteroids observed in the Spitzer data.

The Spitzer Space Telescope observes in four channels corresponding to wavelengths of 3.6$\mu$m, 4.5$\mu$m, 5.8$\mu$m, and 8$\mu$m. The data used in this study is from three areas called dark spot 1, dark spot 2, and dark spot 3. Dark spot 1 is centered at $RA : 13^h45^m33.58^s$ $DEC : +43^d35^m59.8^s$ and covers 0.928 deg$^2$. Dark spot 2 is centered at $RA : 13^h05^m49.68^s$ $DEC : +14^d25^m59.8^s$ and covers 0.953 deg$^2$. Dark spot 3 is centered at $RA : 14^h36^m23.24^s$ $DEC : +67^d46^m18.0^s$ and covers 0.963 deg$^2$. Each dark spot was observed three times, with the separation between observations typically being a few hours. Each observation consisted of many sets of three pictures. The time between the start of the first and second image in each triplet is 46 seconds, the time between the start of the second and third image is 43 seconds. Each dark spot is divided into four quarters. Each quarter is divided into 108 images forming 36 triplets.

## 3. Identifying Asteroids

### 3.1. Finding Candidates in Fits Files

To identify moving objects in the 8$\mu$m Spitzer data an IDL program was used to read through the 108 images that make up each observation of each dark spot quarter, and identify possible asteroids. The background of each image was calculated by measuring the strength of 1000 randomly selected pixels, and taking the mode of that list. One standard deviation higher than the mode was taken as the minimum flux for a source. Using this minimum flux the "Find" function in the IDL Astronomy User's Library generated a list of the pixel coordinates of sources in an image. To calculate the optimum area of the convolution box used by "Find" the strength of ten sources in the first Dark Spot were measured with a circular aperture of varying radius. Sources were chosen that had also been measured by the 2MASS survey at 2.2$\mu$m so the measured strengths could be compared. The strength of the sources was measured with a with radii from 1-5 pixels, every .25 pixels. The radius with the optimum signal to noise ratio would be the one where the source strength stopped being proportional to the radius in pixels squared, and became proportional to the radius. This takes place when the slope of a log plot of the radius vs. source strength passes 1. The radius assigned to the turnover point was the one which generated a slope closest to 1. The mode of the list of optimum radii was 2.75 pixels, so this value was used as the optimum signal to noise aperture radius. However, the "Find" function convolves the image using a square box, not a circle. The area of this convolution box was therefore set to equal the area of the 2.75 pixel radius circle.

The measured strength of each source was also compared to the values given by the 2mass survey. It was assumed that all the flux from a source would have been collected at an aperture radius of 5 pixels. The source strength calculated using a 5 pixel radius was compared to the 2mass measurement of the same source. The average ratio of Measured/2Mass source strengths was 0.112.

With the optimum signal to noise ratio convolution box was being used by "Find," the 36 triplets of images that make up an observation of each dark spot quarter were searched for moving objects. After the list of source coordinates produced by "Find" had been converted from pixel coordinates to Right Ascension and Declination the lists were compared to look for sources that appeared within 5 arcseconds of each other on each of the three images.

### 3.2. Applying Linear and Stationary Fits to the Triplets

Of course the resulting list of candidate triplets contained mostly stationary sources, not the asteroids being looked for. To further narrow down this list, a linear and stationary fit was applied to each triplet. The $\chi^2$ value was calculated for both the stationary and linear fits. To do this, a new set of coordinates based on the "real" right ascension and declination was created. The new coordinates were called $x$ and $y$ and defined as:

$$x = (RA - \overline{RA})\cos(\overline{DEC})$$
$$y = DEC - \overline{DEC}$$

These new coordinates were nearly rectangular and centered on the middle coordinate of each triple. For the purposes of calculating the linear fit, the start time of the first image in each triple was set to $t_1 = 0$. The start times for the subsequent two images were then $t_2 = 46$ and $t_3 = 89$. The average time of each triple was, $\bar{t} = 0$. The difference between each start time and the average time then took on the values $t_i - \bar{t} = -45, 1, 44$. The rate of change of $x$ and $y$ were then calculated, and the results used to generate the linear fit expected values for each point.

$$b_x = \frac{dx}{dt} = \frac{\sum(x_i - \overline{x})(t_i - \bar{t})}{\sum(t_i - \bar{t})^2}$$
$$b_y = \frac{dy}{dt} = \frac{\sum(y_i - \overline{y})(t_i - \bar{t})}{\sum(t_i - \bar{t})^2}$$
$$a_x = \overline{x} - b_x\bar{t}$$
$$a_y = \overline{y} - b_y\bar{t}$$
$$x_{exp} = a_x + b_x t_i$$
$$y_{exp} = a_y + b_y t_i$$

The $\chi^2$ value for the linear fit could then be calculated. Taking $\sigma$ to be 1 for the moment, the linear $\chi^2$ was given by:

$$\chi^2_l = \sum \frac{(x_i - x_{exp})^2 + (y_i - y_{exp})^2}{\sigma_l^2} \quad (1)$$

For the stationary fit the expected values were simply:

$$x_{exp} = \overline{x}$$

$$y_{exp} = \overline{y}$$

The stationary $\chi^2$ was given by:

$$\chi_s^2 = \sum \frac{(x_i - \overline{x})^2 + (y_i - \overline{y})^2}{\sigma_s^2} \tag{2}$$

The next step was to ensure that the average $\chi^2$ value for each fit was equal to the number of degrees of freedom. For the stationary fit, there were four degrees of freedom, for the linear fit there were two. By requiring that $\overline{\chi_l}^2 = 2$ and $\overline{\chi_s}^2 = 4$ the $\sigma$ could be determined for each fit. The $\overline{\chi}^2$ values for the first dark spot was calculated and resulted in $\sigma_l \approx 0.208$" and the $\sigma_s \approx 0.214$". These $\sigma$ values were then put back into the equation so that $\overline{\chi}^2$ would have the appropriate value in each fit.

### 3.3. Confirming Asteroids

With the $\overline{\chi}^2$ values normalized, further requirements could be specified for the candidate triplets. Only triplets which had a $\chi_l^2 < 6$ and $\chi_s^2 - \chi_l^2 > 6$ were written to the IDL program's output file for further examination.

To determine if a candidate source produced by the program was in fact an asteroid, a final check of the images was done by eye. An image of the same location taken during a different observation was viewed. In the time between observations an asteroid would be expected to move well away from its first coordinates. If the source appeared again at the same coordinates, it was dismissed. If the source was not present in the other observation, it was accepted as an asteroid. Figure 1 shows the images of Asteroid 1 used in this process.

As a result of this process two sources were accepted as asteroids. The first, hereafter called Asteroid I, was found in dark spot two. The second, hereafter called Asteroid II, was found in dark spot three. Because Asteroid 2 happened to be on the edge of dark spot three its coordinates were not included in any other observations. However, it was the only source where the difference between the linear and stationary $\chi^2$ values was on par with that of Asteroid I, so it was still accepted as an asteroid despite not being able to check it's coordinates at a different time.

## 4. Properties of Observed Asteroids

The angular speed of each asteroid was measured based on the change in position between the first and third images where it was observed. Asteroid I was actually observed in two consecutive triplets in the same observation, so it was viewed in a total of six images. Asteroid I was only seen in one triplet. The coordinates of asteroids I and II in each image they were observed in is shown in table 1. The angular rate of Asteroid I was $\frac{0.672^\circ}{day}$. The angular rate of Asteroid II was $\frac{0.432^\circ}{day}$.

The flux of Asteroid II was measured in each of Spitzer's four channels. Because Asteroid II was observed on the edge of dark spot three, it was only possible to measure its flux in channels 2 and 4. Planck's law of black-body radiation was used to determine the temperature of the asteroids. Planck's law of black-body radiation is:

$$F_\nu = \Omega \cdot B_\nu(t) \tag{3}$$

$$B_\nu(t) = \frac{2\hbar \cdot \nu^3}{c^2 \cdot (\exp(\frac{h\nu}{kt}) - 1)} \tag{4}$$

Where $F_\nu$ is the flux at a given frequency $\nu$, $\Omega$ is the solid angle of the source, $t$ is the temperature of the black body, $c$ is the speed of light and $k$ is Boltzmann's constant.

Because the flux of Asteroid II could only be measured in two channels, there is only one solution for its temperature and solid angle. The system of two equations using the information for Asteroid II from table 2 results in a temperature of approximately 392°k, and a solid angle of $5.6202 \times 10^{-20} sr$. The flux of Asteroid I was observed in all four of Spitzer's channels, so a better calculation of it's temperature was possible. Solving for $\Omega$ in equation 3 gives:

Table 1. Asteroid Movement

| Object | Image 1 | Image 2 | Image 3 | Image 4 | Image 5 | Image 6 |
|---|---|---|---|---|---|---|
| Asteroid I: | RA:196.30390 | RA:196.30416 | RA:196.30423 | RA:196.30445 | RA:196.30459 | RA:196.30472 |
| | DEC:14.57022 | DEC:14.57027 | DEC:14.57052 | DEC:14.57063 | DEC:14.57071 | DEC:14.5709 |
| Asteroid II: | RA:218.53724 | RA:218.53730 | RA:218.53665 | ··· | ··· | ··· |
| | DEC:67.15233 | DEC:67.15214 | DEC:67.15205 | ··· | ··· | ··· |

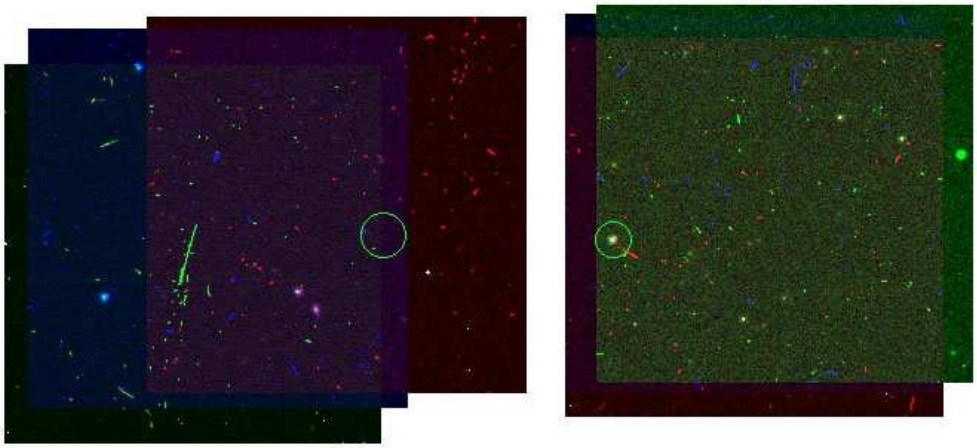

Fig. 1.— Asteroid I is shown in the image on the right. The left image shows the same coordinates a few hours later. These pictures are formed by coloring the first image in the triplet red, the second green, and the third blue, and then superimposing them.

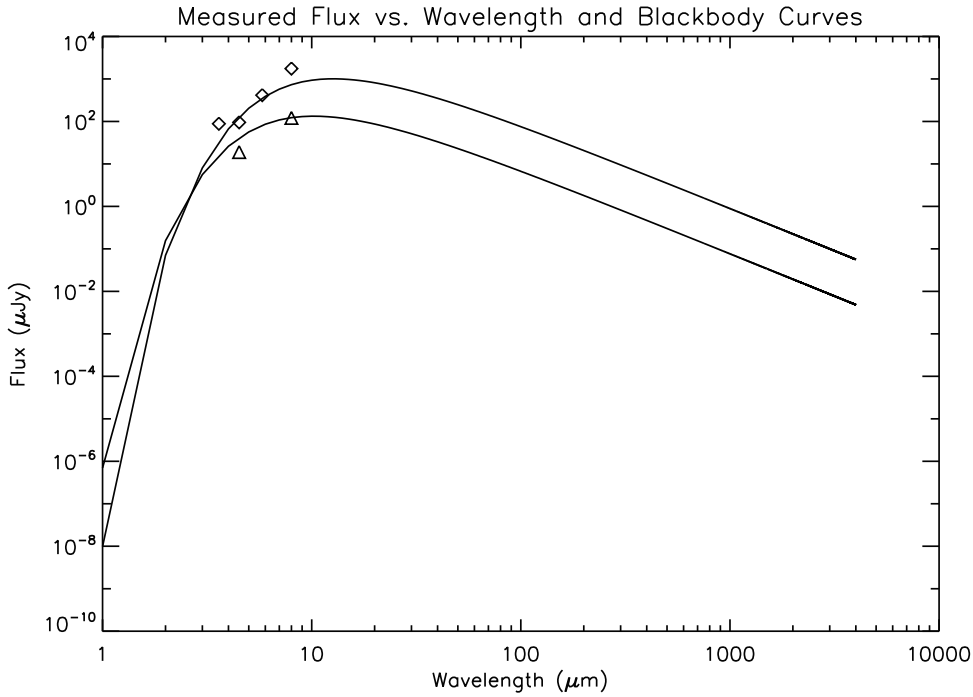


Fig. 2.— On this plot the diamond points are the measured fluxes of asteroid I, and the triangle points are measured fluxes of asteroid II. The curves passing through each set of points are the black body curves corresponding to the calculated temperature and solid angle of each asteroid.

$$\Omega_\nu = \frac{F_\nu}{B_\nu(t)} = \frac{F_\nu c^2(\exp(\frac{h\nu}{kt}) - 1)}{2h\nu^3} \tag{5}$$

The geometric mean of $\Omega$ is given by:

$$< \Omega_\nu >= (\prod_1^4 \Omega_\nu^i)^{\frac{1}{4}} \tag{6}$$

By varying the temperature from 100°-500°$k$ and minimizing $E$ in equation 7

$$E = \sum |\ln(\frac{\Omega_\nu^i}{< \Omega_\nu >})|^2 \tag{7}$$

the best fit values for the temperature and solid angle for Asteroid I were calculated. The resulting temperature was 403°k and the solid angle was $1.2448 \times 10^{-18} sr$.

A list of the 25 asteroids closest to the center of each dark spot during the observation were drawn from Edward Bowell's Asteroid Orbital Elements Database. Using the information provided by the database, the distance from Spitzer to the 25 closest asteroids was calculated. With this data it was possible to estimate the distance from Spitzer to Asteroids I and II. For each dark spot a graph of the angular rate vs. distance to Spitzer of the 25 asteroids was created. The graph's of dark spot 1 and dark spot 2 are shown in figure 3. The distance from Spitzer to Asteroids I and II was estimated based on the range of distances of the 25 asteroids corresponding to the measured angular rate.

Table 2. Asteroid Flux

| Channel/Wavelength ($\mu$m) | Asteroid I Flux ($\mu$Jy) | Asteroid II Flux ($\mu$Jy) |
|---|---|---|
| Channel 1: 3.6 | 1750 | 121 |
| Channel 2: 4.5 | 415 | ··· |
| Channel 3: 5.6 | 95 | 19 |
| Channel 4: 8.0 | 88 | ··· |

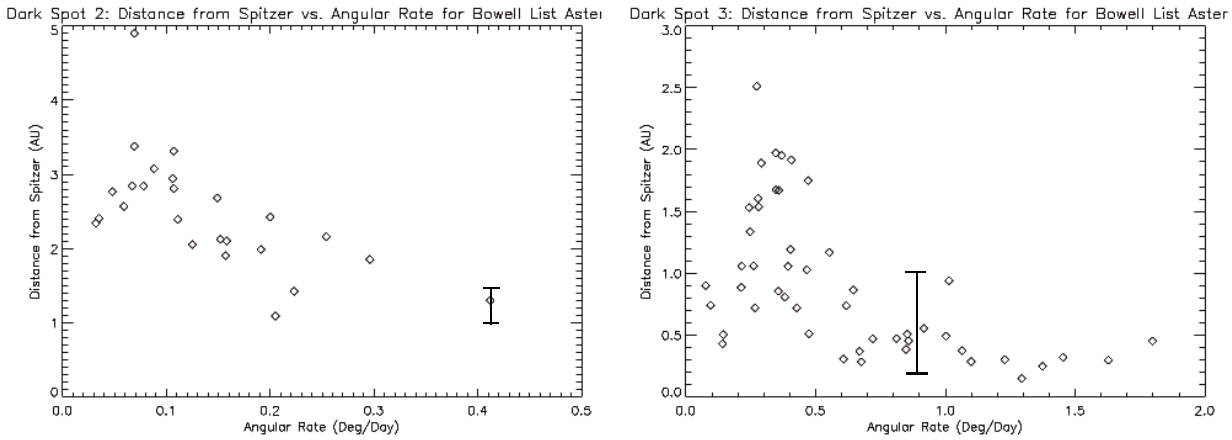


Fig. 3.— A plot of the distance from Spitzer vs. angular rate for the Bowell Asteroids in dark spot 2 is shown on the left, and those from dark spot 3 is shown on the right. Asteroid I is located in dark spot 2, and asteroid II is located in dark spot 3. The bars on the plot show the estimated range of distances corresponding to the angular rate of the respective asteroids.

Using this method the distance from Asteroid I to Spitzer was estimated as being between 1.0-1.5 AU, and the distance from Asteroid II to Spitzer being between 0.2-1.0 AU. With the solid angle of each asteroid already calculated, their sizes could also be calculated according to equation 8.

$$S = \Omega \cdot R^2 = \pi r^2 \tag{8}$$

Where $S$ is the cross sectional surface area of the asteroid, $R$ is the distance between Spitzer and the asteroid and $r$ is the radius of the asteroid. By using the estimated distances between Spitzer and the asteroids in equation 8 the diameter of Asteroid I was calculated to be 188-283m. The diameter of Asteroid II was calculated to be 16-40m.

A summary of the information determined about Asteroids I and II is given in table 3.

## 5. Comparison of Results to Existing Models

To compare these results to the number of asteroids per square degree predicted by other models it was necessary to determine the flux sensitivity in each dark spot. To do

this, the flux of every source being registered by "Find" was measured and displayed in a histogram. The histogram bin where the frequency of sources is at a maximum corresponds to the lowest flux that can be reliably detected. Figure 4 shows these histograms. In dark spot 1 the sensitivity was 200$\mu$Jy, in dark spot two the sensitivity was 500$\mu$Jy, and in dark spot 3 the sensitivity was 100$\mu$Jy.

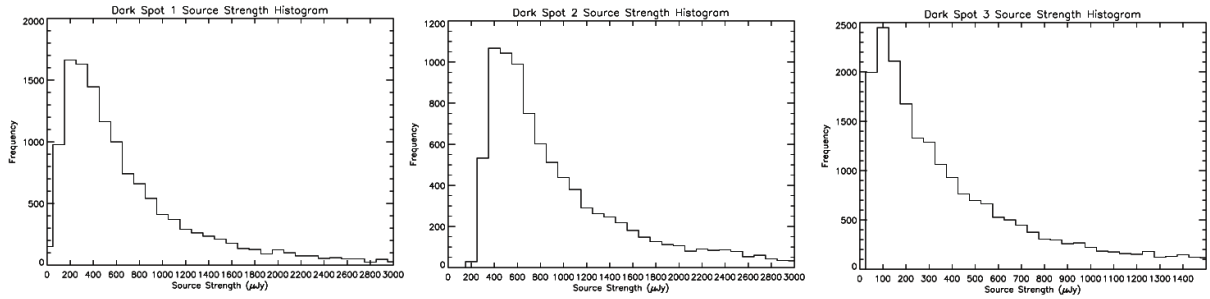


Fig. 4.— These histograms show the frequency of source flux for each dark spot. The bin where frequency is at a maximum gives an estimate of the lowest source flux that can be reliably detected. For dark spot one this is 200$\mu$Jy, for dark spot 2 this is 500$\mu$Jy, and for dark spot 3 this is 100$\mu$Jy.

The minimum diameter of a detectable asteroid is calculated according to equation 9 where $R_s$ is the distance between the asteroid and the sun, and $F8at1km@1Au$ is the flux measured from a 1km diameter asteroid at a distance of 1 AU.

$$d = R_s \times \sqrt{\frac{Sensitivity}{F8at1km@1AU}} \tag{9}$$

For a given model the number of asteroids with a diameter greater than D depends on the total population of asteroids and a power P, specified by the model according to equation 10.

$$N > D = (Population) \times (\frac{1km}{D})^P \tag{10}$$

To predict how many asteroids would be expected in the dark spots observed, the Bowell list was used again. For each of the 25 asteroids closest to the center of a given dark

Table 3. Summary of Asteroid Information

| Source | Angular Rate (Deg/Day) | Estimated Distance to Spitzer (AU) | Speed (meters/second) | Ω | Diameter (meters) | Temperature (kelvin) |
|---|---|---|---|---|---|---|
| Asteroid I | .432 | 1.0-1.5 | 13055-19582 | $1.2448\times10^{-18}sr$ | 188-282 | 403 |
| Asteroid II | .672 | 0.2-1.0 | 4062-20308 | $5.6202\times10^{-20}sr$ | 16-40 | 392 |

spot the minimum detectable diameter was calculated using the sensitivity measured in that dark spot. The Bowell list contains 336,326 asteroids and their orbits. The population number to use in equation 10 was then $(TotalPopulation)/(336,326)$. Plugging in the minimum detectable diameter from equation 9 into equation 10 generates $N_t$, the total number of detectable asteroids predicted by the model. The number of asteroids per degree, $N_{deg}$, is then calculated by dividing $N_t$ by the area covering the 25 Bowell list asteroids. That area is equal to $\pi(\theta_{max})^2$, where $\theta_{max}$ is the angular distance from the center of the dark spot of the furthest asteroid. For the asteroids with angular rates of greater than $1"/89s$ the predicted $N_{deg}$'s were summed up to get the total expected $N_{deg}$.

For the Ivezic paper the total population of asteroids with diameters greater than 1 km is estimated to be $7 \times 10^5$, and P is 1.3 (Ivezic et al. 2002). Using the method described above with the measured sensitivity in each region this predicts 0.78 asteroids in dark spot 1, 0.75 asteroids in dark spot 2, and 0.88 asteroids in dark spot 3. For the Tedesco paper the total population is estimated to be $1.9 \times 10^6$ and P is 2.3 (Tedesco et al. 2005). This predicts 33.05 asteroids in dark spot 1, 2.8 asteroids in dark spot 2, and 85.77 in dark spot 3.

Using the Bowell list in this fashion has an observational bias in the population of asteroids used, but with only two objects being found it is probably not a large error. It is evident that the number of asteroids observed agrees very closely with the number of asteroids with diameters greater than 1 km predicted by the Ivezic model, and differs greatly from the predictions of the Tedesco model in dark spots 1 and 3.

## 6. Acknowledgments

I would like to thank Prof. Edward Wright for his guidance and help with every stage of this research, and Louis Levenson who was of invaluable assistance with problems big and small. I would also like to thank the National Science Foundation for funding the REU program during which this research was conducted.

## REFERENCES

Evans R., et al. 1998, Icarus Volume 131 pp. 264-185. Asteroid Trails in Hubble Space Telescope.

Tedesco, E., & Cellino, A., Zappala, V. 2005, AJ, 129:2869-2886. The Statistical Asteroid Model. I. The Maine Belt Population For Diameters Greater than 1 Kilometer.

Ivezic,Z., Juric, M., Lutpon, R., Tabachnik, S., & Quinn, T., 2002, astro-ph/0208099, Asteroids Observed by The Sloan Digital Sky Survey.